Sensors

Deutsche Ausgabe: DOI: 10.1002/ange.201607195
Internationale Ausgabe: DOI: 10.1002/anie.201607195

Exceptionally Selective and Tunable Sensing of Guanine Derivatives and Analogues by Structural Complementation in a G-Quadruplex

Xin-min Li, Ke-wei Zheng, Yu-hua Hao, and Zheng Tan**

Abstract: *A guanine-vacancy-bearing G-quadruplex (GVBQ) interacts with guanine and derivatives by a structural complementation to form a more stable and intact G-quadruplex. Sensors using GVBQs are devised to detect guanine and other nucleobases, and their derivatives derived from structurally similar compounds. A strict requirement of Hoogsteen hydrogen bonds between the GVBQ and analyte in the structural complementation confers exceptional selectivity on the analyte. As such, subtle modifications on analytes affecting even a single hydrogen bond can preclude the recognition. In principle, the strategy may also be expanded to detect many planar cyclic compounds. Because nucleobases and derivatives/metabolites are involved in many physiological and pathological processes, this type of sensor may find applications in risk assessment of pathogenesis and therapeutics related to nucleic acid metabolism.*

Nucleobases and derivatives play an essential role in cellular physiology, except for serving as coding elements in DNA and RNA. Taking guanine as an example, the binding of GTP/GDP to the G-proteins regulates signal transmission across the cytoplasm membrane and consequently manipulates many cellular activities.[1] Abnormal levels of nucleobases and their metabolites reflect disorders in nucleic acid metabolism which leads to a variety of diseases, such as cancer, immunodeficiency, aging, kidney diseases, gout, and several mitochondrial pathologies.[2] For example, the urinary level of the guanine metabolites 8-oxo-2′-deoxyguanosine (8-Oxo-2′-dG) and 8-oxo-2′-deoxyguanine (8-Oxo-2′-G) are biomarkers of DNA oxidative damage,[3] a consequence of cellular metabolism that plays a major role in mutagenesis, carcinogenesis, and aging.[4] It has been shown that nuclear oxidative damage is associated with poor survival in colorectal cancer[5] and urinary 8-Oxo-2′-dG has been used as a predictor of survival in patients treated with radiotherapy.[6] 8-Oxo-2′-dG and 8-Oxo-2′-G have also being regarded as molecular markers of cancer.[7] The rapid proliferation of tumor cells correlates with a significantly higher cellular concentration of nucleotides, including GTP. On the other hand, guanine nucleotide depletion triggers cell cycle arrest and apoptosis.[8] In addition, nucleoside analogues have been widely used in antitumor and antivirus therapies.[9] For these reasons, the detection of nucleobases and derivatives provides valuable information in the metabolic and pathological status, therapeutic responses, and DNA modifications of an individual.

In the past decade, fluorimetric and colorimetric sensors have been actively developed for the nucleotide of the four main nucleobases, namely adenine, uracil/thymine, cytosine, and guanine.[10] They display change in either intensity or wavelength in either fluorescence emission or absorbance to indicate the presence and amount of analyte. Because of the high chemical and structural similarity among these target molecules, many of these sensors suffer poor discrimination among the nucleobases and some response to other anionic compounds. While most of these sensors are intended for adenine derivatives, such as ATP, very few targeted GTP.[11]

Herein we report an exceptionally selective sensing strategy for the detection of guanine and its derivatives using a guanine-vacancy-bearing G-quadruplex (GVBQ) as a sensing element. A GVBQ carries a guanine vacancy (G-vacancy) at one of the G-quartet layers, and it can be filled by a guanine to complete an intact G-quartet (Figure 1 A).[12] To sense guanine, a DNA oligonucleotide is labeled with a fluorescent dye at one end and a quencher at the other. The DNA sequence is designed to potentially form either a hairpin or a GVBQ. Without analyte, the hairpin is favored to keep the dye and quencher close to each other so that the fluorescence is quenched. In the presence of guanine base, the G-vacancy in the GVBQ is filled to promote the formation and stabilization of the G-quadruplex. As such, the hairpin opens and the dye is set apart from the quencher by a bulky G-quadruplex and an oligonucleotide tail, thus giving rise in fluorescence to signal the presence and concentration of the analyte (Figure 1 B).

We first used a G3332 DNA with three G_3 and one G_2 tracts in the G-core and a FAM dye/BHQ1 quencher pair (Table 1). G-quadruplexes are stabilized by K^+ but not by Li^+.[13] The circular dichroism (CD) spectrum of the DNA showed a positive peak at $\lambda = 265$ nm and negative one at $\lambda =$

[*] Dr. X.-m. Li, Dr. K.-w. Zheng, Y.-h. Hao, Prof. Dr. Z. Tan
State Key Laboratory of Membrane Biology
Institute of Zoology, Chinese Academy of Sciences
Beijing 100101 (P. R. China)
E-mail: zhengkewei@ioz.ac.cn
z.tan@ioz.ac.cn

Supporting information and the ORCID identification number(s) for the author(s) of this article can be found under http://dx.doi.org/10.1002/anie.201607195.

Table 1: Probe DNA sequences.

Probe	Sequence (5′—3′)[a]
G3332	FAM-tagggtgGGCTGGGAGGTTTTTTTTTTcacccta-BHQ1
X3233[b]	TGG**X**CGGAGGGAAGTgggataTTTtatccc-TAMRA
O3233[c]	TGGGCGGAGG**O**AAGTgggataTTTtatccc-TAMRA

[a] Complementary regions are indicated by lowercase letters. G-tracts are underlined. Modified nucleobases aimed to fit targeted analytes are shown in bold font. [b] X = xanthosine. [c] O = 8-Oxo-2′-dG.

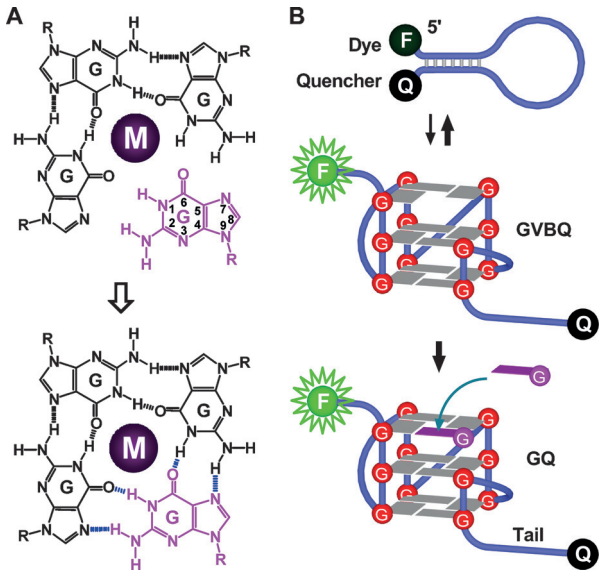

Figure 1. Illustration of detection of guanine and its derivatives by structural complementation between GVBQ and the analyte. A) An intact G-quadruplex is composed of a few layers of G-quartets in which guanine bases are held together by Hoogsteen hydrogen bonds (blue dashed line) and stabilized by a metal ion, such as K^+. B) A probe DNA is designed to form either a hairpin using two complementary regions near the two ends or a GVBQ with a G-vacancy in one of the G-quartets. Hairpin is favored in the absence of guanine. A fluorescent dye (F) attached at one end of the DNA is quenched by a quencher (Q) at the other end in the hairpin. A guanine base in solution can fill the G-vacancy to stabilize the formation of G-quadruplex. The conversion of hairpin into G-quadruplex (GQ) separates the dye from the quencher, by a G-quadruplex and an oligomer tail, and restores fluorescence.

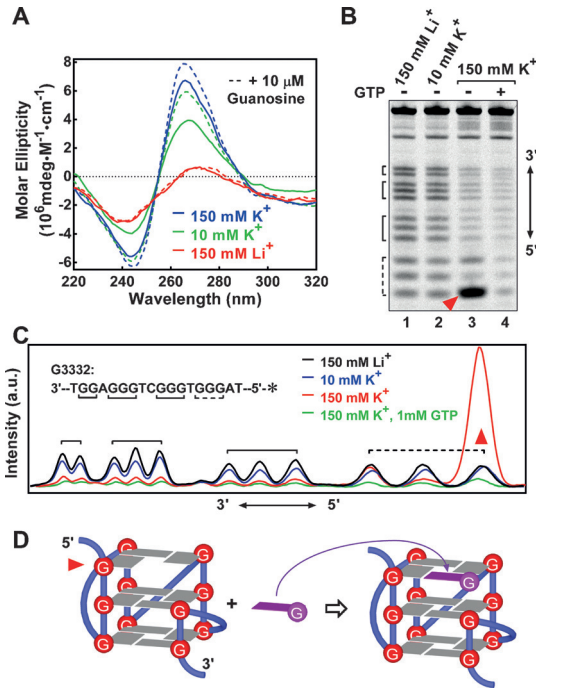

Figure 2. GVBQ formation in G3332 DNA and guanine fill-in detected by CD spectroscopy (A) and DMS footprinting (B). A) CD spectra obtained in the absence and presence of 10 μM guanosine in solution containing the indicated concentration of cations. B) DNA cleavage fragments resolved by denaturing gel electrophoresis. C) Digitization of the gel in B. D) Scheme of derived GVBQ structure and G-quartet completion by G fill-in in the GVBQ. Brackets in B–C indicate G-tract and red arrowhead in B–D indicates the hypercleaved guanine residue which was protected by a G fill-in with GTP in 150 mM K^+.

245 nm in 150 mM K^+ (Figure 2A, blue curve), thus suggesting it formed a parallel G-quadruplex. To enhance its responsiveness to guanine, we reduced the K^+ to 10 mM, which resulted in a similar spectrum with a reduced magnitude at the two peaks (green curve). An addition of guanosine led to an increase at $\lambda = 265$ nm and a decrease at $\lambda = 245$ nm in 150 and 10 mM K^+, respectively, thus implying a fill-in of guanine into and stabilization of the GVBQ in both solutions (dashed blue and green curves). This fill-in was dependent on the G-quadruplex structure because it was not seen in a Li^+ solution (solid versus dashed red curve) in which formation of G-quadruplexes is not favored.

The formation of a GVBQ and guanine fill-in was verified by dimethyl sulfate (DMS) footprinting, a test of G-quadruplex formation by the protection of guanine residues in a G-quadruplex against chemical cleavage.[14] In 150 mM Li^+, all the guanine residues in the guanine tracts (G-tracts) suffered significant cleavage (Figure 2B, lane 1; Figure 2C, black curve). They were slightly protected in 10 mM K^+ (Figure 2C, blue curve), thus suggesting that the GVBQ started to form. When the K^+ concentration was raised to 150 mM to fully stabilize the GVBQ, the cleavage at the three G-tracts from the 3′ side were dramatically reduced, while a hypercleavage occurred in the first G-tract from the 5′ side (Figures 2B and 2C, red arrowhead). According to our previous work, this hypercleavage represents attack at the exposed N7 of the guanine base beside the G-vacancy. It completely disappeared when GTP was supplied to fill-in the G-vacancy (Figure 2C, green curve), as expected.[12] The CD spectra and DMS footprint pattern for 150 mM K^+ agreed with a folding topology illustrated in Figure 2D.[12]

Because 10 mM K^+ was intended to be used for G3332 to leave room for the analyte-induced hairpin-to-G-quadruplex conversion (Figure 1B), we further tested if the GVBQ was indeed formed and able to accept a guanine in this solution. The DNA was incubated with a trifunctional compound, sulfosuccinimidyl-2-[6-(biotinamido)-2-(*p*-azidobenzamido) hexanoamido]ethyl-1,3′-dithiopropionate (SBED)-GMP (see Figure S1 in the Supporting Information), and irradiated with UV-light. Once the guanine group in this compound fills a G-vacancy in the GVBQ, UV-irradiation can induce a covalent crosslinking between its phenyl azide group and the primary amines in either the adenine, guanine, or cytosine residues in DNA.[12] Figure 3A shows a denaturing gel analysis of the UV-irradiated samples. An extra slow-migrating band in lanes 6 and 9 showed occurrence of crosslinking and is indicative of a guanine fill-in at both 10 and 150 mM K^+. Because the compound also carried a biotin moiety, which can bind a streptavidin, the extra bands were shifted further by streptavidin in native gel electrophoresis (Figure 3B, lanes 6 and 9). In contrast, little crosslinking was detected for the DNA in Li^+ solution (Figures 3A,B, lane 3).

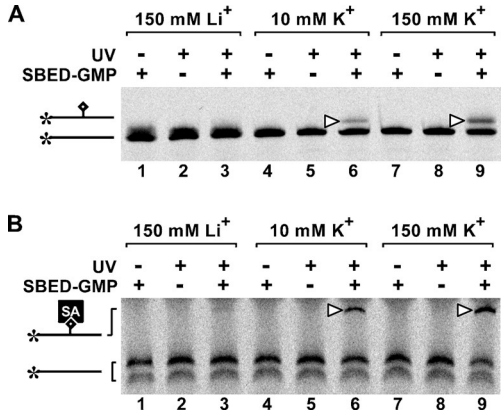

Figure 3. Confirmation of G fill-in in the GVBQ of G3332 DNA by photo-crosslinking and subsequent electrophoretic mobility shift. A) Crosslinking between SBED-GMP and G3332 DNA detected by denaturing gel electrophoresis. B) Mobility shift of crosslinked G3332 DNA by streptavidin (SA) detected by native gel electrophoresis. Schemes at the left side of gel indicate the structure of the corresponding DNA bands. Open triangle indicates crosslinked DNA. The two bands at the bottom of gel may present hairpin and GVBQ, respectively.

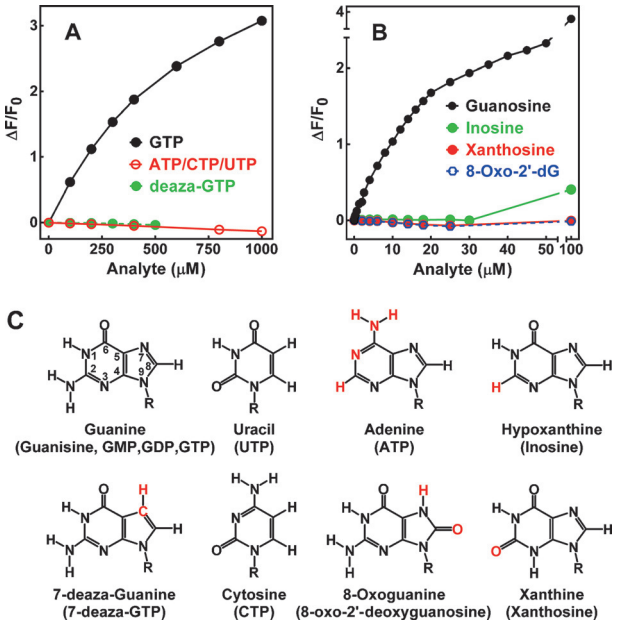

Figure 4. Detection of GTP and guanosine by G3332 DNA depicted by the fractional increase in fluorescence ($\Delta F/F_0$) as a function of analyte concentration. Here F_0 is the fluorescence in the abscence of analyte and ΔF the change in fluorescence upon addition of analyte. A) Detection of GTP and discrimination against 7-deaza-GTP and a mixture of ATP, CTP, and UTP each at the indicated concentration. B) Detection of guanosine and discrimination against inosine, xanthosine, and 8-Oxo-2′-dG. C) Nucleobases of corresponding analytes (within parentheses) examined. Modifications in comparison to guanine are in red.

The aforementioned results demonstrate that an unstable GVBQ formed in G3332 DNA in 10 mM K^+ has the capability to accept a guanine. To test its responsiveness to analytes, we incubated the DNA with guanosine and examined the fluorescent emission of the FAM dye. The increase in fluorescence upon guanosine addition (see Figure S2) provides support that a structural conversion (Figure 1B) occurred, as expected. We then incubated the DNA with GTP, a mixture of ATP/CTP/UTP, and a GTP analogue, 7-deaza-GTP, and examined, respectively, the fluorescence emission. The GVBQ demonstrated excellent selectivity among the nucleobases (Figure 4A). An increase in fluorescence was only found with GTP, which is able to fill-in the G-vacancy in the GVBQ (black curve). No signal was observed for the mixture of ATP/CTP/UTP (red curve). Compared with the normal GTP, N7 of the base is replaced by a carbon atom in 7-deaza-GTP. This single-atom substitution prevents the Hoogsteen hydrogen bond from forming at N7 and totally precluded the fluorescence signal (green curve).

The discrimination of the GVBQ against 7-deaza-GTP implied that the Hoogsteen hydrogen bonds were essential for the recognition of an analyte. We then tested four other guanine derivatives with subtle modifications at the base. The results in Figure 4B indicate that the GVBQ only interacted with the guanosine as expected. Virtually no signal showed up for the other derivatives below a concentration of 30 μM, with modification affecting merely one Hoogsteen hydrogen bond. For example, a single hydrogen atom at N7 of the 8-oxoguanine base in the 8-Oxo-2′-dG (Figure 4C) totally precluded the recognition (Figure 4B). The formation of the GVBQ and selectivity towards the guanine base was further confirmed by DMS footprinting (see Figure S3), in which the G-tracts were protected only with GTP and guanosine, but not with the other derivatives.

In Figure 4, it was noted that the guanosine was detected with a much greater sensitivity than was the GTP (Figure 4A versus 4B, black curve) since it does not have the three negative charges as does GTP and, therefore, suffered no static electric repulsion. This fact suggested that guanine nucleotides could be discriminated against by the number of charges they bear. A test with GMP, GDP, and GTP (Figure 5) showed that with an increase in their negative charge from zero to three, the fluorescence signal decreased accordingly.

Nucleobase derivatives are also widely used in anticancer and antiviral medication. We further tested two guanine analogue drugs, Ganciclovir and Acyclovir, by using the

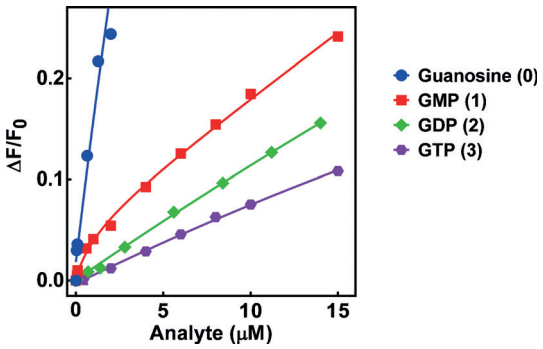

Figure 5. Detection by G3332 DNA of four guanine derivatives bearing different numbers of phosphates which can be negatively charged. Number of phosphates is indicated within parentheses at the right side of each analyte.

G3332 sensor (Figure 6). They are charge-free and showed sensitivity similar to that of guanosine. Again, a promotion of GVBQ formation by the two drugs was verified by DMS footprinting (see Figure S4).

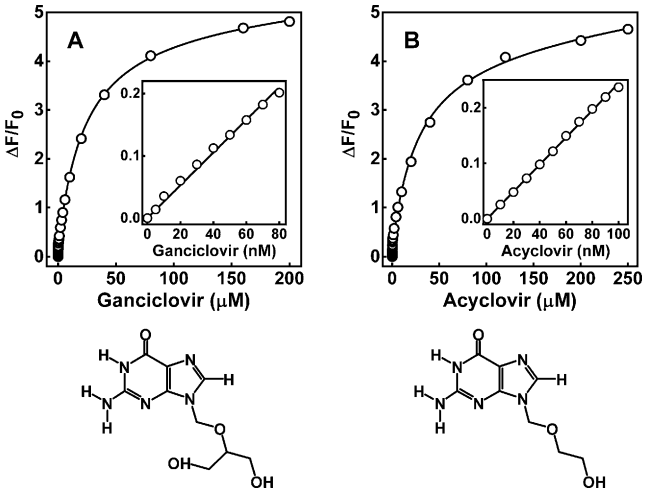

Figure 6. Detection by G3332 DNA of A) Ganciclovir and B) Acyclovir. Insert shows linearity at low analyte concentration taken from the main graph.

The structural complementation not only detects guanine bases and derivatives, but it can also be expanded to detect modified guanine bases as long as a proper formation of Hoogsteen hydrogen bonds is arranged in a G-quartet to accommodate the fill-in of an intended analyte. To exemplify this ability, we show here how a GVBQ can be modified to detect 8-Oxo-2′-dG, a biomarker of DNA oxidative damage,[3] as well as xanthosine.

For 8-Oxo-2′-dG, we used an X3233 DNA labeled with a TAMRA dye at the 3′ end (Table 1). The DNA sequence was arranged to form a triad layer containing a xanthosine, which permits Hoogsteen hydrogen bonding with an 8-oxoguanine base in a G-quartet (Figure 7A).[15] A quencher was not used since the supplier was unable to make more than two modifications on the probe. In this case, the TAMRA dye was quenched by the proximal guanine bases in the opposite strand by photoinduced electron transfer when the DNA formed a hairpin (Figure 7B).[16] Similar to G3332, the CD spectrum of this DNA suggested it formed a parallel G-quadruplex, which was enhanced by the intended 8-Oxo-2′-dG, thus resulting in an elevated peak magnitude at both $\lambda =$ 245 and 265 nm (see Figure S5A, red versus black curve), but not affected by guanosine and xanthosine (green and blue curves). In agreement with this, the DMS footprinting showed that 8-Oxo-2′-dG enhanced the stability of the GVBQ as revealed by the better protection of the guanines in the G-tracts (see Figures S5B and S5C).

The interaction of 8-Oxo-2′-dG with the GVBQ in the X3233 DNA was successfully detected by an increase in the fluorescence from the TAMRA (Figure 7C). The signal was specific to 8-Oxo-2′-dG (black curve) and the fluorescence showed little change when the DNA was incubated with guanosine and xanthosine (red and green curve).

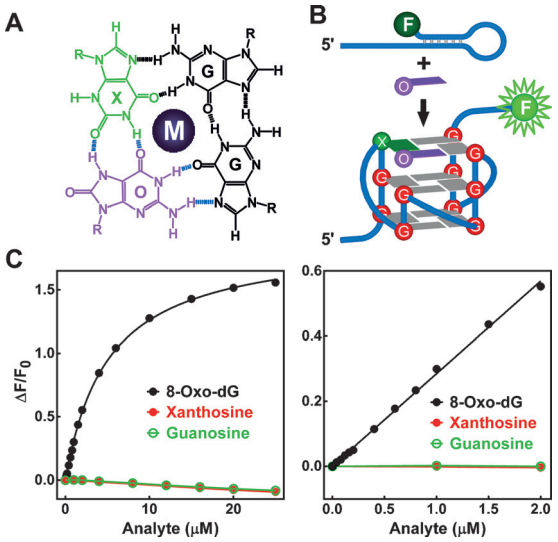

Figure 7. Detection of 8-Oxo-2′-dG in comparison with guanosine and xanthosine by X3233 DNA. A) Schematic structure of a xanthosine-modified G-quartet with a filled-in 8-Oxo-2′-dG (O). B) Assumed hairpin to GVBQ conversion induced by 8-Oxo-2′-dG in X3233 DNA. C) Fluorescence change as a function of analyte concentration.

From Figure 7A, it was deduced that the same base quartet could be used to sense xanthosine if an 8-oxoguanine base could be instead incorporated into the DNA (Figure 8A). Thus we synthesized an O3233 DNA containing 8-Oxo-2′-dG at the end of the third G-tract (Table 1). Similarly, its CD spectrum (see Figure S6) suggested that the DNA formed a parallel G-quadruplex (Figure 8B). We carried out DMS footprinting for this DNA and were unable to detect protection of the guanine residues because of a serious cleavage at 8-Oxo-2′-dG. In spite of this, the data in Figure 8C showed that O3233 was able to selectively detect xanthosine,

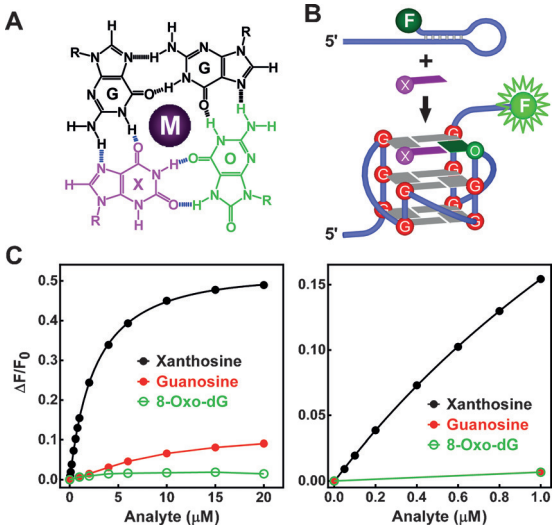

Figure 8. Detection of xanthosine in comparison with guanosine and 8-Oxo-2′-dG by O3233 DNA. A) Schematic structure of an 8-Oxo-2′-dG-modified G-quartet with a filled-in xanthosine (X). B) Assumed hairpin to GVBQ conversion induced by xanthosine in O3233 DNA. C) Fluorescence change as a function of analyte concentration.

although with a reduced sensitivity compared with that of the X3233 DNA with the 8-Oxo-2′-dG.

From the aforementioned experiments, it is seen that the recognition of GVBQ by its analyte is mainly based on the Hoogsteen hydrogen bonds between the GVBQ and analyte within the dedicated G-quartet layer. In addition, the stacking between the G-quartet layers favors planar analytes. Because of these requirements, the recognition of a guanine base has achieved excellent specificity and interactions with the other nucleobases are nearly negligible. This selectivity is in contrast to the two recently reported GTP sensors for which the signal generated by ATP was about one-third to one-half of that produced by GTP.[11a,c]

In addition to the strict selection among nucleobases, GVBQ also discriminates analytes from the same origin by the number of charges they bear, as illustrated by G3332 (Figure 5). This property may be useful for profiling and separating the contents of a mixture of derivatives of guanine or nucleobases using GVBQ as an affinity ligand in separation techniques such as chromatography. For example, GVBQ may be used as a stationary phase to capture all guanine derivatives at high salt concentration. The captured analytes may then be eluted according to the charges they carry by, for instance, a salt gradient. This approach would be very useful in handling complex mixtures because it offers an additional and highly specific selection at the loading stage to exclude non-relevant components prior to analyte separation. As a more specific example, total guanine nucleotides (TGN) have been used in pathological, metabolic, and toxicology assessment.[17] The G3332 sensor may well be suited to detect TGN. In this case, the charges of the guanine species can be shielded by high salt concentration such that they are all selectively and effectively recognized.

The structural complementation is not limited to the sensing of guanine and derivatives, but can be extended to sense other guanine analogues such as 8-Oxo-2′-dG and xanthosine with the same or similar selectivity (Figures 7 and 8). In principle, the sensing strategy is potentially applicable to other nucleobases or similar cyclic planar compounds if a proper planar molecular quartet can be arranged in a G-quadruplex. Such tunable structural complementation may offer a more general platform for sensing and separating nucleobases and certain cyclic planar compounds, and for detecting modifications on these compounds.

As a "proof-of-principle" study with little optimization, our results already demonstrate sensitivity ranging from a few tens of nanomolar to micromolar concentration of analytes with exceptional selectivity. Improvement in sensitivity and selectivity is expected if optimization can be carried out. For example, the detection sensitivity of the O3233 and X3233 DNA may greatly benefit from quenching of the TAMRA dye. In their current form, the two probes have a much higher background signal than the G3332, thus yielding a lower signal in response to their analyte. With appropriate fluorogenesis and a dedicated quartet, analyte sensing will depend on an appropriate competition between the formation of the hairpin and the GVBQ. In the absence of an analyte, the sensor DNA should be mainly in the form of a hairpin, so the fluorophore can be efficiently quenched, and it can also be turned into a G-quadruplex in the presence of analyte. There are several parameters which may be used to optimize this conversion, such as stem length, number of G-quartet layers, and loop size in both the hairpin and GVBQ. Besides, changes in anion species and concentration, the ratio of K^+ over Li^+ can manipulate the stability of both hairpin and GVBQ. A fine adjustment on the equilibrium between the hairpin and GVBQ in a desired direction may be further made with polyethyleneglycol (PEG), which has been shown to destabilize DNA duplexes and stabilize G-quadruplexes.[18]

Experimental Section

GVBQ characterization and analyte detection were conducted in 50 mM Lithium cacodylate buffer (pH 7.4) containing 140 mM Li^+, 10 mM K^+, and 40% PEG 200 for G3332, or 50 mM Li^+, 100 mM K^+, and 40% PEG 200 for X3233, or 90 mM Li^+, 60 mM K^+, and 50% PEG 200 for O3233, unless otherwise indicated. Fluorescence was measured and expressed as fractional change in intensity. Excitation and emission wavelength was set at $\lambda = 488$ and 520 nm, respectively, for FAM-labeled DNA; $\lambda = 556$ and 579 nm, for TAMRA-labeled DNA. Supporting figures and more experimental details are provided in the Supporting Information.

Acknowledgments

This work was supported by MSTC (grants 2013CB530802 and 2012CB720601) and NSFC (grants 31470783 and 21432008).

Keywords: DNA · G-quadruplexes · hydrogen bonds · nucleic acids · sensors

How to cite: *Angew. Chem. Int. Ed.* **2016**, *55*, 13759–13764
Angew. Chem. **2016**, *128*, 13963–13968

[1] S. R. Neves, P. T. Ram, R. Iyengar, *Science* **2002**, *296*, 1636–1639.
[2] K. M. Aird, R. Zhang, *Cancer Lett.* **2015**, *356*, 204–210.
[3] R. Olinski, R. Rozalski, D. Gackowski, M. Foksinski, A. Siomek, M. S. Cooke, *Antioxid. Redox Signaling* **2006**, *8*, 1011–1019.
[4] R. De Bont, N. van Larebeke, *Mutagenesis* **2004**, *19*, 169–185.
[5] J. Sheridan, L. M. Wang, M. Tosetto, K. Sheahan, J. Hyland, D. Fennelly, D. O'Donoghue, H. Mulcahy, J. O'Sullivan, *Br. J. Cancer* **2009**, *100*, 381–388.
[6] K. Roszkowski, R. Olinski, *Cancer Epidemiol. Biomarkers Prev.* **2012**, *21*, 629–634.
[7] K. Roszkowski, W. Jozwicki, P. Blaszczyk, A. Mucha-Malecka, A. Siomek, *Med. Sci. Monit.* **2011**, *17*, CR329–333.
[8] a) T. W. Traut, *Mol. Cell. Biochem.* **1994**, *140*, 1–22; b) J. Laliberté, A. Yee, Y. Xiong, B. S. Mitchell, *Blood* **1998**, *91*, 2896–2904; c) E. Messina, P. Gazzaniga, V. Micheli, M. R. Guaglianone, S. Barbato, S. Morrone, L. Frati, A. M. Agliano, A. Giacomello, *Int. J. Cancer* **2004**, *108*, 812–817.
[9] L. P. Jordheim, D. Durantel, F. Zoulim, C. Dumontet, *Nat. Rev. Drug Discovery* **2013**, *12*, 447–464.
[10] Y. Zhou, Z. Xu, J. Yoon, *Chem. Soc. Rev.* **2011**, *40*, 2222–2235.
[11] a) N. Wu, J. Lan, L. Yan, J. You, *Chem. Commun.* **2014**, *50*, 4438–4441; b) S. Wang, Y. T. Chang, *J. Am. Chem. Soc.* **2006**, *128*, 10380–10381; c) P. P. Neelakandan, M. Hariharan, D. Ramaiah, *J. Am. Chem. Soc.* **2006**, *128*, 11334–11335; d) S. K. Kim, B.-S. Moon, J. H. Park, Y. I. Seo, H. S. Koh, Y. J. Yoon, K. D. Lee, J. Yoon, *Tetrahedron Lett.* **2005**, *46*, 6617–6620; e) J. Y. Kwon,

N. J. Singh, H. N. Kim, S. K. Kim, K. S. Kim, J. Yoon, *J. Am. Chem. Soc.* **2004**, *126*, 8892 – 8893.
[12] X. M. Li, K. W. Zheng, J. Y. Zhang, H. H. Liu, Y. D. He, B. F. Yuan, Y. H. Hao, Z. Tan, *Proc. Natl. Acad. Sci. USA* **2015**, *112*, 14581 – 14586.
[13] C. C. Hardin, A. G. Perry, K. White, *Biopolymers* **2000**, *56*, 147 – 194.
[14] D. Sun, L. H. Hurley, *Methods Mol. Biol.* **2010**, *608*, 65 – 79.
[15] a) V. V. Cheong, B. Heddi, C. J. Lech, A. T. Phan, *Nucleic Acids Res.* **2015**, *43*, 10506 – 10514; b) V. V. Cheong, C. J. Lech, B. Heddi, A. T. Phan, *Angew. Chem. Int. Ed.* **2016**, *55*, 160 – 163; *Angew. Chem.* **2016**, *128*, 168 – 171.
[16] a) M. Torimura, S. Kurata, K. Yamada, T. Yokomaku, Y. Kamagata, T. Kanagawa, R. Kurane, *Anal. Sci.* **2001**, *17*, 155 – 160; b) C. P. Vaughn, K. S. Elenitoba-Johnson, *Am. J. Pathol.* **2003**, *163*, 29 – 35.
[17] a) I. Baranowska-Bosiacka, A. J. Hlynczak, *Biol. Trace Elem. Res.* **2004**, *100*, 259 – 273; b) W. Dudzinska, A. Lubkowska, B. Dolegowska, K. Safranow, K. Jakubowska, *Eur. J. Appl. Physiol.* **2010**, *110*, 1155 – 1162; c) W. Dudzinska, A. J. Hlynczak, *Diabetes Metab.* **2004**, *30*, 557 – 567.
[18] a) K. W. Zheng, Z. Chen, Y. H. Hao, Z. Tan, *Nucleic Acids Res.* **2010**, *38*, 327 – 338; b) Y. Xue, Z. Y. Kan, Q. Wang, Y. Yao, J. Liu, Y. H. Hao, Z. Tan, *J. Am. Chem. Soc.* **2007**, *129*, 11185 – 11191; c) Z. Y. Kan, Y. Lin, F. Wang, X. Y. Zhuang, Y. Zhao, D. W. Pang, Y. H. Hao, Z. Tan, *Nucleic Acids Res.* **2007**, *35*, 3646 – 3653.

Received: July 25, 2016
Revised: September 11, 2016
Published online: October 7, 2016

